Sixth International Symposium on Turbulence and Shear Flow Phenomena
Seoul, Korea, 22-24 June 2009

COHERENT VORTEX SIMULATION (CVS) OF A 3D COMPRESSIBLE TURBULENT MIXING LAYER

Olivier Roussel*
Institut für Technische Chemie und Polymerchemie,
Universität Karlsruhe (TH),
Kaiserstr. 12, 76128 Karlsruhe,
Germany

Kai Schneider
M2P2–CNRS & CMI,
Université de Provence,
39 rue Joliot-Curie, 13453 Marseille Cedex 13,
France,
kschneid@cmi.univ-mrs.fr

ABSTRACT

An adaptive multiresolution method based on a second order finite volume discretization is presented for solving the three-dimensional compressible Navier–Stokes equations in Cartesian geometry. The explicit time discretization is of second order and for the flux evaluation a 2–4 Mac Cormack scheme is used. Coherent Vortex Simulations (CVS) are performed by decomposing the flow variables into coherent and incoherent contributions. The coherent part is computed deterministically on a locally refined grid using the adaptive multiresolution method, while the influence of the incoherent part is neglected. The computational efficiency of this approach, in terms of memory and CPU time compression, is illustrated for a turbulent mixing layer in the weakly compressible regime. A comparison with direct numerical simulation allows to assess the precision and efficiency of CVS.

INTRODUCTION

The numerical simulation of fully-developed turbulent flows in the incompressible and even more in the compressible regime is still a challenging task in computational fluid dynamics. The difficulty comes from the nonlinear dynamics of the Navier–Stokes equations, which excite a very large range of temporal and spatial scales. To perform computations in industrially relevant configurations, turbulence models are necessary because Direct Numerical Simulation (DNS) of fully–developed turbulent flows is up to now, and in the near future, limited to low Reynolds numbers. However, most turbulence models used in industrial codes are based on phenomenology, and thus require tuning of their parameters for each flow configuration.

Multiscale and multiresolution methods for modeling and computing turbulent flows have become more and more fashionable, also for compressible flows, due to their efficiency and improved fidelity with respect to classical approaches. An overview can be found in the book of Sagaut and coworkers (2006) or in a forthcoming review article by Schneider & Vasilyev (2010).

The Coherent Vortex Simulation (CVS), which is based on a multiresolution decomposition, has been introduced by Farge, Schneider and coworkers (1999, 2001) for modeling incompressible turbulent flows. The flow is split into coherent and incoherent contributions by means of an orthogonal wavelet filtering of the vorticity field. The coherent flow is then computed deterministically, while the influence of the incoherent background flow is statistically modelled or neglected.

For incompressible isotropic turbulence, it was shown by Okamoto et al. (2007), that the number of degrees of freedom N required for CVS grows slower with the Reynolds number Re, i.e. $N \propto Re^{3.9}$, than for DNS where Kolmogorov-type arguments imply $N \propto Re^{4.5}$. This motivates the development of CVS for computing fully developed turbulent flows. Hereby adaptive space discretizations are essential to be able to benefit from the efficient representation of the coherent flow to be computed, in terms of memory and CPU time savings.

In Roussel et al. (2003) we presented an efficient adaptive multiresolution method for evolutionary PDEs, which is in the currect work applied to the compressible Navier–Stokes equtions for advancing the coherent flow components on a dynamically adaptive grid.

In the following, we present CVS computations of a weakly compressible mixing layer and compare the results with a DNS reference run. For further details, we refer the reader to Roussel & Schneider (2009).

COMPRESSIBLE NAVIER–STOKES EQUATIONS

We consider the three-dimensional compressible Navier–Stokes equations in a domain $\Omega \subset \mathbb{R}^3$. Using Einstein's summation convention, the balance equations in Cartesian coordinates can be written in the following dimensionless form,

$$\begin{aligned} \frac{\partial \rho}{\partial t} &= -\frac{\partial}{\partial x_j}\left(\rho\, u_j\right) \\ \frac{\partial}{\partial t}\left(\rho\, u_i\right) &= -\frac{\partial}{\partial x_j}\left(\rho\, u_i\, u_j + p\, \delta_{i,j} - \tau_{i,j}\right) \\ \frac{\partial}{\partial t}\left(\rho\, e\right) &= -\frac{\partial}{\partial x_j}\left(\left(\rho\, e + p\right)\, u_j - u_i\, \tau_{i,j} - \lambda \frac{\partial T}{\partial x_j}\right) \end{aligned} \qquad (1)$$

where ρ, p,T and e denote the dimensionless density, pres-

*Present address: Universidade Estadual de Campinas, IMECC, Caixa Postal 6065, 13083–970 Campinas, SP, Brazil

sure, temperature and specific total energy per unit of mass, respectively, and $(u_1, u_2, u_3)^T$ is the dimensionless velocity vector. The components of the dimensionless viscous strain tensor $\tau_{i,j}$ are

$$\tau_{i,j} = \frac{\mu}{Re}\left(\frac{\partial u_i}{\partial x_j} + \frac{\partial u_j}{\partial x_i} - \frac{2}{3}\frac{\partial u_k}{\partial x_k}\delta_{i,j}\right) , \qquad (2)$$

where μ denotes the dimensionless molecular viscosity and Re the Reynolds number. The dimensionless conductivity λ is defined by

$$\lambda = \frac{\mu}{(\gamma - 1)\ Ma^2\ Re\ Pr} , \qquad (3)$$

where γ, Ma and Pr respectively denote the specific heat ratio and the Mach and Prandtl numbers.

The system is completed by an equation of state for a calorically ideal gas

$$p = \frac{\rho\, T}{\gamma\ Ma^2} . \qquad (4)$$

and suitable initial and boundary conditions.

Assuming the temperature to be larger than 120 K, the molecular viscosity varies with the temperature according to the dimensionless Sutherland law

$$\mu = T^{\frac{3}{2}}\left(\frac{1\ +\ T_s}{T\ +\ T_s}\right) \qquad (5)$$

where $T_s \approx 0.404$.

Denoting by (x, y, z) the three Cartesian directions, this system of equations can be written in the following compact form

$$\frac{\partial U}{\partial t} = -\frac{\partial F}{\partial x} - \frac{\partial G}{\partial y} - \frac{\partial H}{\partial z} \qquad (6)$$

where $U = (\rho,\ \rho u_1,\ \rho u_2,\ \rho u_3,\ \rho e)^T$ denotes the vector of the conservative quantities, and F, G, H are the flux vectors in the directions x, y, and z, respectively.

CVS METHOD

In this section, we present an extension of the CVS method to compressible flows. The CVS method is based on the observation that turbulent flows contain both an organized part, the coherent vortices, and a random part, the incoherent background flow. The separation into coherent and incoherent contributions is done using a non-linear wavelet filtering. As for compressible flows both vortical and potential components are present, we decompose the conservative variables $U = (\rho,\ \rho u_1,\ \rho u_2,\ \rho u_3,\ \rho e)$ into a biorthogonal wavelet series by applying the cell-average multiresolution transform described in Harten (1995).

First the dimensionless density and pressure are decomposed into

$$\begin{aligned} \rho &= \rho_C + \rho_I , \\ p &= p_C + p_I . \end{aligned} \qquad (7)$$

where ρ_C and p_C respectively denote the coherent part of the density and pressure fields, while ρ_I and p_I denote the corresponding incoherent parts.

Then the other remaining variables, i.e. the velocity components u_1, u_2, u_3, the temperature T and energy e, are decomposed using the Favre averaging technique, i.e., density weighted, as done in RANS and LES of compressible flows to simplify modeling. For a quantity φ corresponding to one of these remaining variables, we obtain the following decomposition,

$$\varphi = \varphi_C + \varphi_I \ , \text{ where } \varphi_C = \frac{(\rho\varphi)_C}{(\rho)_C} \qquad (8)$$

Finally, retaining only the coherent contributions of the conservative variables we obtain the filtered compressible Navier–Stokes equations which describe the flow evolution of the coherent flow U_C.

The evolution of the coherent flow U_C is computed in physical space using a finite volume scheme on a locally refined grid, while the incoherent contributions U_I are discarded during the flow evolution, which models turbulent dissipation. To discretize the convective terms in space and time, we use a 2–4 McCormack scheme (Gottlieb & Turkel, 1976), while the diffusive terms are discretized using a second–order centered scheme in space and an explicit second–order Runge–Kutta scheme in time. The wavelet basis used for the filtering relies on the cell–average multiresolution analysis developed by Harten (1995). After the filtering, the discarded coefficients are removed from memory, so that both CPU time and memory requirements are significantly reduced in comparison with the DNS computation. The data structure is organized into a graded-tree form to be able to navigate through it. To perform the CVS computations, a three–dimensional adaptive multiresolution algorithm (Roussel et al. 2003), originally developed for reaction–diffusion equations, has been extended to the compressible Navier–Stokes equations. Extensions of the adaptive multiresolution scheme to the compressible Euler equations can be found in Domingues et al. (2009). Local scale–dependent time stepping was investigated in Domingues et al. (2008), which allows a further speed–up of space–adaptive schemes.

NUMERICAL RESULTS

As example, we apply the CVS method here to compute a time–developing three–dimensional turbulent mixing layer in the weakly compressible regime. CVS computations of incompressible turbulent mixing layers have been presented in Schneider et al. (2005). In this test-case, both layers have the same initial velocity norm, but oposite directions. An initial three-dimensional sinusoidal perturbation is added to the basic profile. The flow configuration is depicted in Fig. 1. The maximal resolution of the computation is 128^3, which corresponds to $L = 7$ scales. The computational domain is a three–dimensional cube $\Omega = [-30, 30]^3$ and the final time of all computations corresponds to $t = 80$. Periodic boundary conditions are applied for the x- and y-directions and Neumann conditions are imposed in the z-direction. The Prandtl and Mach numbers are set to 0.71 and 0.3 respectively, whereas the specific heat ratio γ equals 1.4. The CFL number is set to 0.4. The Reynolds number based on the initial velocity norm and half the initial layer thickness yields 200. The CVS result is compared with the one obtained by DNS performed on the regular finest grid with the same numerical scheme (Table 1). We find that only 17.9 % wavelet coefficients contain around 98.3 % of the energy and 93.4 % of the enstrophy. Taking into account all the nodes of the tree data structure, these wavelet coefficients represent 30.2 % of the $128^3 = 2097152$ cells that the fine–grid computation requires. Concerning the CPU time, it only represents 29.0 % of the one required by the DNS, i.e., CVS is in the present case three times faster than DNS.

Isosurfaces of vorticity, shown in Fig. 2 (top), illustrate

Table 1: Comparison between DNS and CVS of a 3D compressible mixing layer, $Ma = 0.3, Re = 200$. CPU time required on a Pentium IV 2.5 GHz, percentages of CPU time, required memory, total energy E and total enstrophy Z in comparison with the DNS computation.

Method	% CPU	% Mem	% E	% Z
DNS	100.0 %	100.0 %	100.0 %	100.0 %
CVS	29.0 %	30.2 %	98.3 %	93.4 %

the flow evolution. At $t \approx 19$, the Kelvin–Helmholtz instability generates four rollers in the streamwise direction. At the beginning, the mixing layer remains approximately two–dimensional, later on, the vortices begin to pair so that, at $t \approx 37$, we observe two vortex pairings. At $t \approx 78$, these two pairings are finished and three–dimensional structures appear, generated by the oblique mode between the two remaining vortices. For longer computational times, assuming that the domain is sufficiently large, these two vortices would pair again, thus leading to only one vortex. The adaptive grid in Fig. 2 (bottom) shows that the adaptive multiresolution method automatically tracks the flow evolution. To compare the the CVS results with the DNS reference computation we plot in Fig. 3 the evolution of energy (left), enstrophy (center) and of the streamwise energy spectrum at the final time instant (right). The CVS and DNS spectra are in good accordance except for smallest scales, i.e., for $k > 10$, where a slight difference between CVS and DNS can be observed. The time evolution of energy and enstrophy (Fig. 3, left and center) confirm the good agreement between the CVS and DNS computations, keeping in mind that CVS requires around one third of the CPU time and the memory required by the DNS (Table 1).

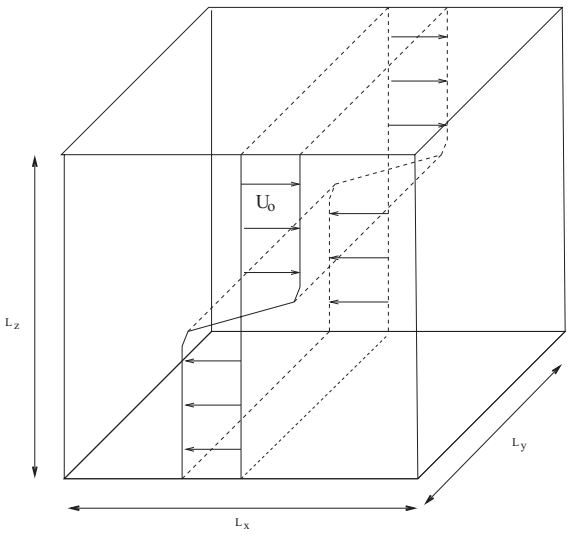

Figure 1: Flow configuration: domain and initial basic flow $\mathbf{u}_0$ of the three–dimensional mixing layer.

CONCLUSIONS

The above computations for a three–dimensional weakly compressible mixing layer show that the CVS method yields accurate results in comparison with DNS, while reducing the CPU time and memory requirements by around a factor three. Further work will focus on the CVS of compressible mixing layers with larger values of both Mach and Reynolds numbers, i.e., in a more turbulent and more compressible regime, for which higher compression of memory and CPU time are expected, cf. Domingues et al. (2009).

ACKNOWLEDGMENTS

We thankfully acknowledge financial support from the French *Agence Nationale pour la Recherche* (project M2TFP)and the French–German CNRS–DFG program "LES of complex flows". K.S. also acknowledges partial financial support from the Institut Carnot STAR.

REFERENCES

Domingues, M., Gomes, S., Roussel, O., and Schneider, K., 2009, "Space–Time adaptive multiresolution methods for hyperbolic conservation laws: Applications to compressible Euler equations", *Appl. Num. Math.*, in press.

Domingues, M., Gomes, S., Roussel, O., and Schneider, K., 2008, "An adaptive multiresolution scheme with local time–stepping for evolutionary PDEs", *J. Comput. Phys.*, 227:3758–3780.

Farge, M., 1992, "Wavelet transforms and their applications to turbulence", *Annu. Rev. Fluid Mech.*, 24:395–458.

Farge, M., Schneider, K., and Kevlahan, N., 1999, "Non-gaussianity and coherent vortex simulation for two–dimensional turbulence using and adaptive orthonormal wavelet basis", *Phys. Fluids*, 11(8):2187–2201.

Farge, M., and Schneider, K., 2001, "Coherent Vortex Simulation (CVS), a semi–deterministic turbulence model using wavelets", *Flow, Turbul. Combust.*, 66(4):393-426.

Gottlieb, D., and Turkel, E., 1976, "Dissipative two–four methods for time–dependent problems", *J. Comput. Phys.*, 30:703-723.

Harten, A., 1995, "Multiresolution algorithms for the numerical solution of hyperbolic conservation laws", *Comm. Pure Appl. Math.*, 48:1305-1342.

Okamoto, N., Yoshimatsu, K., Schneider, K., Farge, M., and Kaneda, Y., 2007, "Coherent vortices in high resolution DNS of homogeneous isotropic turbulence: a wavelet viewpoint", *Phys. Fluids*, 19(115109):1–13.

Roussel, O., and Schneider, K., 2009, "Coherent Vortex Simulation for weakly compressible turbulent mixing layers using adaptive multiresolution methods", *J. Comput. Phys.*, under revision.

Roussel, O., Schneider, K., Tsigulin, A., and Bockhorn, H., 2003, "A conservative fully adaptive multiresolution algorithm for parabolic PDEs", *J. Comput. Phys.*, 188(2):493–523.

Sagaut, P., Deck, S., and Terracol, M., 2006, *Multiscale and multiresolution approaches in turbulence.* Imperial College Press.

Schneider, K., Farge, M., Pellegrino, G., and Rogers, M., 2005, "Coherent vortex simulation of 3D turbulent mixing layers using orthogonal wavelets", *J. Fluid Mech.*, 534:39–66.

Schneider, K., and Vasilyev, O., 2010, "Wavelet methods in Computational Fluid Dynamics", *Annu. Rev. Fluid Mech.*, Vol. 42, to appear.

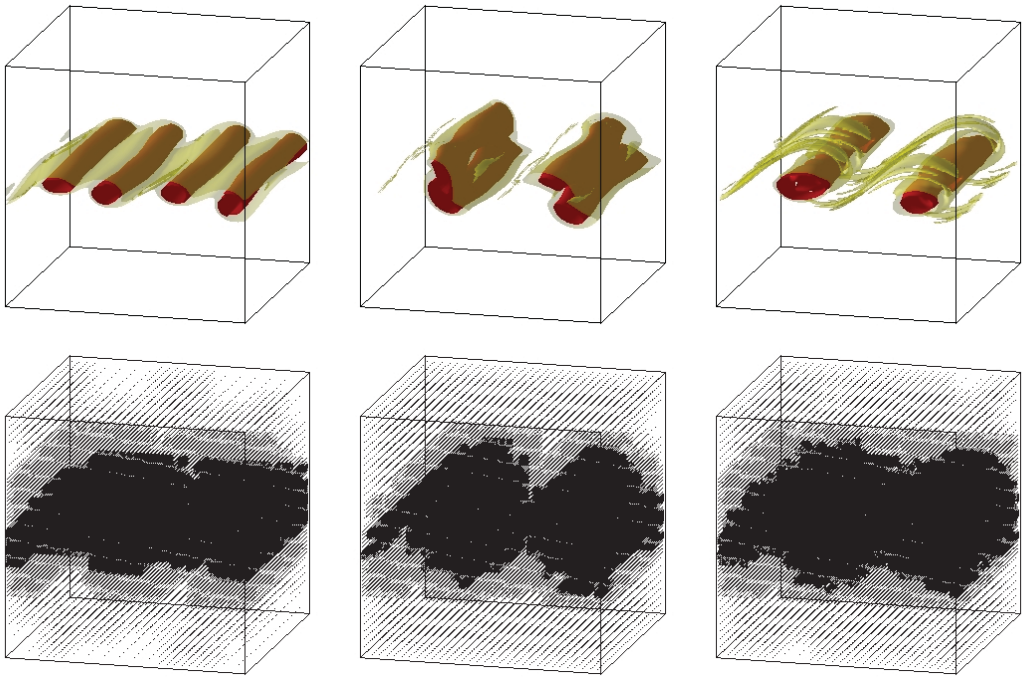

Figure 2: CVS of a 3D weakly compressible mixing layer, $Ma = 0.3, Re = 200$. Top: isosurfaces of vorticity $\| \omega \| = 0.6$ (black) and $\| \omega \| = 0.4$ (gray) at $t = 18$ (left), $t = 37$ (center), and $t = 80$ (right). Bottom: corresponding adaptive grids.

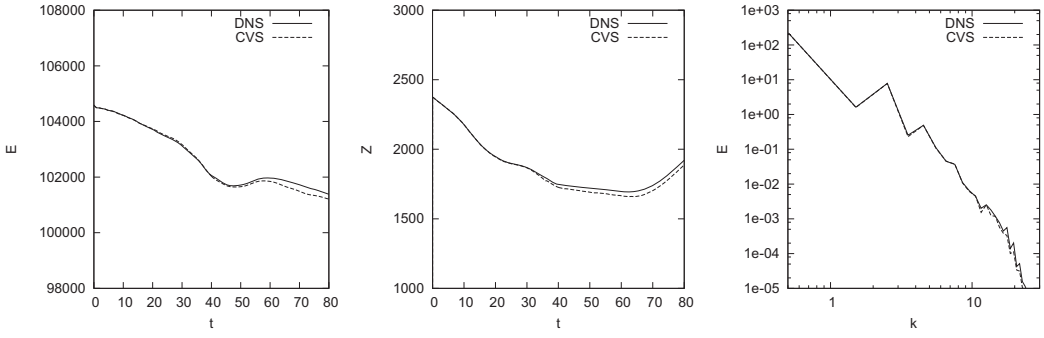

Figure 3: Comparison between DNS and CVS for a 3D weakly compressible mixing layer, $Ma = 0.3, Re = 200$. Left: time evolution of kinetic energy E. Center: time evolution of enstrophy Z. Right: energy spectra in the streamwise direction at $t = 80$.